

Biomimetic Kinetic Resolution: Highly Enantio- and Diastereoselective Transfer Hydrogenation of Aglain Ketones To Access Flavagline Natural Products

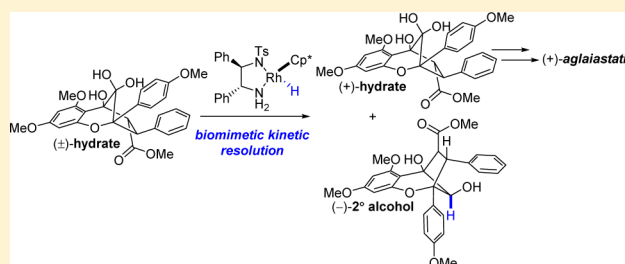
Steven D. Stone,^{‡,†} Neil J. Lajkiewicz,^{‡,†} Luke Whitesell,[‡] Ahmed Hilmy,[‡] and John A. Porco, Jr.*^{‡,†}

[‡]Department of Chemistry and Center for Molecular Discovery (BU-CMD), Boston University, Boston, Massachusetts 02215, United States

[†]Whitehead Institute for Biomedical Research (WIBR), Cambridge, Massachusetts 02142, United States

S Supporting Information

ABSTRACT: We have previously reported asymmetric syntheses and absolute configuration assignments of the aglains (+)-ponapensin and (+)-elliptifoline and proposed a biosynthetic kinetic resolution process to produce enantiomeric rocaglamides and aglains. Herein, we report a biomimetic approach for the synthesis of enantiomerically enriched aglains and rocaglamides via kinetic resolution of a bridged ketone utilizing enantioselective transfer hydrogenation. The methodology has been employed to synthesize and confirm the absolute stereochemistries of the pyrimidone rocaglamides (+)-aglaiastatin and (–)-aglaroxin C. Additionally, the enantiomers and racemate of each metabolite were assayed for inhibition of the heat-shock response, cytotoxicity, and translation inhibition.



INTRODUCTION

Plants of the genus *Aglaiia* are known to produce a variety of unique secondary metabolites including the cyclopenta[*b*]-benzofurans methyl rocaglate (**1**),¹ aglaiastatin (**2**),² and aglaroxin C (**3**)^{2b,3} and the cyclopenta[*b,c*]benzopyran (aglain) ponapensin (**4**)⁴ (Figure 1). These metabolites and derived synthetic analogues thereof have been reported to have potent antitumor,^{2–5} anti-inflammatory,⁶ neuroprotective,⁷ cardiopro-

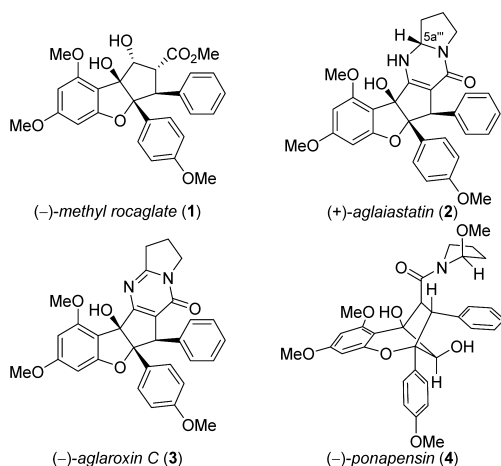


Figure 1. Aglain and rocaglate natural products. Absolute stereochemistries are shown for **1** and **4**; relative stereochemistries are depicted for **2** and **3**.

TECTIVE,⁸ and serine hydrolase inhibitory activities.⁹ The natural product families are proposed¹⁰ to arise from a common aglain intermediate. From previous work in our laboratory assigning the absolute stereochemistry of (–)-ponapensin (**4**),^{11a} it was determined that rocaglates/rocaglamides and the aglains (–)-ponapensin (**4**) and (–)-elliptifoline¹¹ arise from intermediates with opposite absolute configuration.

In previous studies, we proposed^{11a} that ketoreductase or reductoisomerase enzymes¹² could differentiate between the enantiomers of ketone **5a**, selecting for either direct reduction or rearrangement followed by reduction as part of a parallel kinetic resolution¹³ process (Figure 2). In the case of kinetic resolution of aglain ketone **5a**, both enantiomers may be converted to bioactive natural products which led us to investigate the application of a reductive, chemical kinetic resolution approach to enantiopure ketone **5a**.

Noyori and co-workers have previously used chiral ruthenium complexes in the kinetic resolution of racemic secondary alcohols.¹⁴ Metz and co-workers¹⁵ recently demonstrated the utility of this approach for the reductive, kinetic resolution of racemic flavanone substrates. Herein, we report the kinetic resolution of aglains such as **5a** via reduction of a chiral, racemic bridged ketone and its application toward the total syntheses of the pyrimidones (+)-aglaiastatin (**2**) and (–)-aglaroxin C (**3**).

Received: November 14, 2014

Published: December 17, 2014

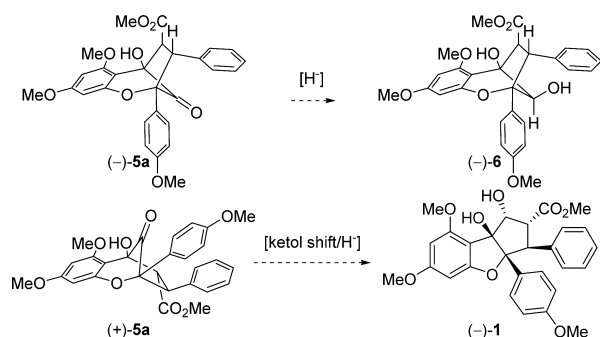
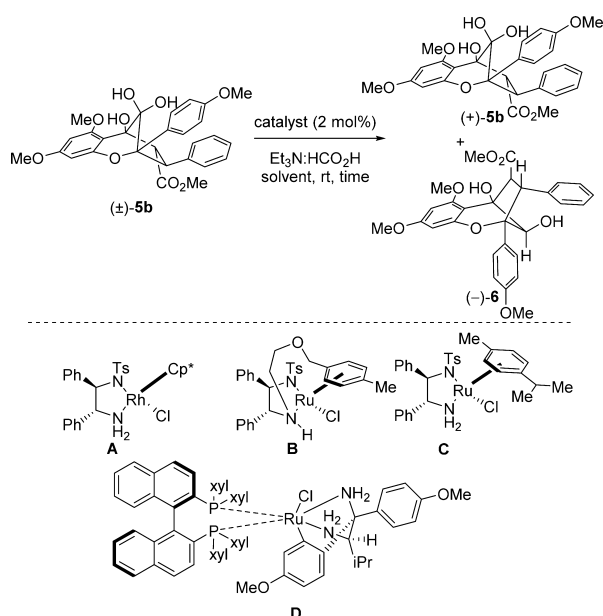


Figure 2. Proposed biosynthetic kinetic/parallel kinetic resolution to access both natural product families.

RESULTS AND DISCUSSION

Biomimetic Kinetic Resolution. Our initial investigations utilized conditions recently reported by Metz and co-workers¹⁵ for asymmetric transfer hydrogenation of racemic flavanones via Rh (III) catalysis employing hydrate **5b**^{11a} which to our delight afforded (–)-**6** in 95% ee after 40% conversion (Table 1, entry 1). The absolute stereochemistry was determined through comparison to (+)-**6**, previously assigned through X-ray crystal structure analysis and synthesis of (–)-methyl rocaglate from a common intermediate.^{11a} Even after a more than 5-fold increase in reaction time (entry 2), we could not push the reaction to 50% conversion. After further optimization, CH₂Cl₂

Table 1. Metal and Ligand Screen for Catalytic, Asymmetric Reduction



entry	catalyst	solvent	time, h	conv (ee), %
1	A	EtOAc	3	40 (95)
2	A	EtOAc	16	40 (96)
3	A	EtOAc ^a	6	trace
4	A	THF	3.5	43 (95)
5	A	CH ₂ Cl ₂	5	50 (96)
6	B	CH ₂ Cl ₂	5	63 (69)
7	C	CH ₂ Cl ₂	5	60 (43)
8	D	CH ₂ Cl ₂	5	nr

^a4 Å molecular sieves used.

was found to be the solvent of choice, providing optimal conversion (entry 5). Low conversions observed (entries 1, 2, and 4) were likely due to the insolubility of hydrate **5b** in both ethyl acetate and THF. *In situ* dehydration of **5b** with 4 Å molecular sieves (entry 3) led to no reaction, suggesting that the molecular sieves were interfering with the process. Furthermore, subjecting of ketone **5a** to the reaction conditions did not produce significantly different results from use of hydrate **5b**. Other metal hydride and ligand systems were tested (entries 6–8), each affording lower enantioselectivity or in one case no reactivity (entry 8).

What was perhaps more intriguing than the excellent enantioselectivity was the complete diastereoselectivity observed. Based on our previous reductions of ketone **5a** and hydrate **5b**,^{11a} we hypothesized that non-coordinating reducing agents would preferably attack the *in situ* generated ketone away from the phloroglucinol ring. Since the rhodium catalyst system is sterically encumbered, we believe that other modes of stabilization enhance attack from the phloroglucinol face. In the aforementioned example of kinetic resolution of flavanones through catalytic asymmetric transfer hydrogenation, Metz and co-workers¹⁵ proposed an assembly for kinetic resolution of flavanones featuring stabilizing CH–π interactions¹⁶ between the methyl groups on the Cp* ligand and the aromatic substituent of the ketone. Figure 3 depicts models generated

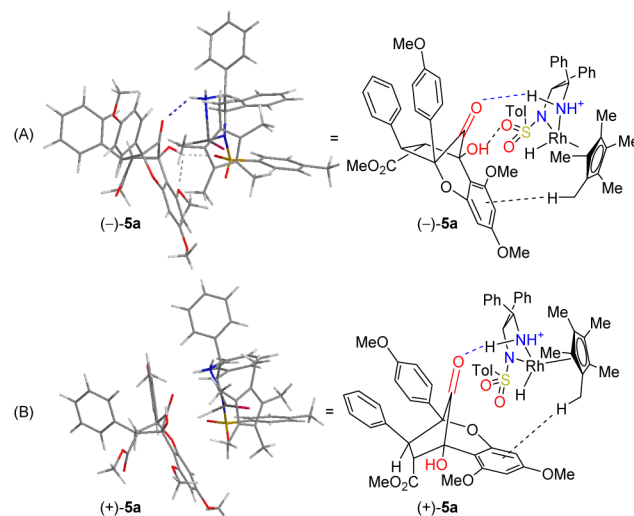


Figure 3. Proposed models for the favored (A) and disfavored (B) diastereomeric assemblies.

using Spartan '10¹⁷ for both favored and disfavored enantiomers of aglain ketone substrates. In the case of the favored substrate/catalyst assembly (Figure 3A) we propose that, in addition to the stabilizing CH–π interaction, a hydrogen bond between the tertiary alcohol of substrate (–)-**5a** and the sulfonyl oxygen of the catalyst helps to direct the chiral reducing agent. In the case of the disfavored substrate/catalyst (Figure 3B), this hydrogen bond interaction is not evident which allows (–)-**5a** to be selectively reduced through assembly A. This is in contrast to the assembly proposed by Metz and co-workers in which a destabilizing steric interaction led to selective reduction of one enantiomer.¹⁵

To evaluate the scope of the kinetic resolution on different substrates, we synthesized a variety of aglain ketone analogs and subjected them to the optimized conditions (Table 2). Our aim was to manipulate the electronics of the aromatic system and

Table 2. Substrate Scope for Reduction

Kinetic resolution:

substrate

(±)-5b: R₁ = R₂ = OMe

(±)-7: R₁ = R₂ = H

(±)-9: R₁ = OMe, R₂ = Br

(±)-10: R₁ = F, R₂ = OMe

(±)-8

catalyst **A** (2 mol%)
HCO₂H/Et₃N
CH₂Cl₂, rt, 5 h

reduced product

(-)-6: R₁ = R₂ = OMe

(-)-11: R₁ = R₂ = H

(-)-12: R₁ = OMe, R₂ = Br

(-)-13: R₁ = F, R₂ = OMe

catalyst **A** (2 mol%)
HCO₂H/Et₃N
CH₂Cl₂, rt, 5 h

Ketol shift/reduction:

(±)-5b: R₁ = R₂ = OMe

(±)-7: R₁ = R₂ = H

(±)-9: R₁ = OMe, R₂ = Br

(±)-10: R₁ = F, R₂ = OMe

1. NaOMe, MeOH
2. Me₄NBH(OAc)₃

(-)-1: R₁ = R₂ = OMe

(-)-14: R₁ = OMe, R₂ = Br

(-)-15: R₁ = F, R₂ = OMe

entry	substrate	conv, %	ee of reduced product (yield), %	ee of starting material ^a (yield), %
1	(±)-5b	50	96 (45)	>99 (42)
2	(±)-7	20	78 (16)	19 (22)
3	(±)-8	n.r.	N/A	N/A
4	(±)-9	47	>99	88
5	(±)-10	37	74 (13)	41 (31)

^aFor entries 1, 4, and 5, enantioenriched starting material was converted to the corresponding (–)-rocaglate derivatives via ketol shift/reduction (*vide supra*) to measure ee. For entry 2, enantioenriched (+)-7 was converted to reduced product (+)-11.

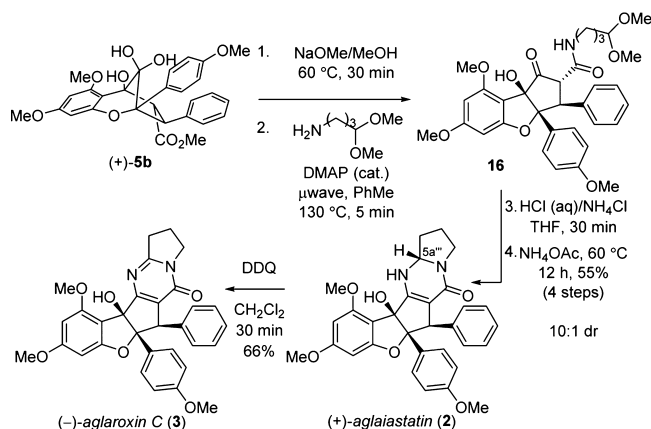
^aFor entries 1, 4, and 5, enantioenriched starting material was converted to the corresponding (–)-rocaglate derivatives via ketol shift/reduction (*vide supra*) to measure ee. For entry 2, enantioenriched (+)-7 was converted to reduced product (+)-11.

observe its effect on the kinetic resolution. Desmethoxy substrate 7 produced both a lower conversion and decreased enantioselectivity (entry 2). When the aryl ring was not directly adjacent to the reactive ketone, the reaction did not occur as demonstrated by attempted reduction of β-keto ester 8 (Table 2, entry 3). Results using the 4'-Br-substituted derivative 9¹⁸ are identical to that of the trimethoxy system suggesting that the substitution of the aryl group coplanar to the ketone has little effect. Difluorinated substrate 10¹⁹ led to an erosion of ee more so than the desmethoxy system. This is likely due to the less electron rich π system being unable to form a strong CH–π bond with the Cp* ligand²⁰ thus slowing conversion. To evaluate the ee of the starting materials, the isolated material was converted to methyl rocaglate analogs 14 and 15. Enantioenriched (+)-7 was directly reduced to (+)-11 using NaBH(OAc)₃.^{11a}

Total Syntheses of (+)-Aglaiaastatin and (–)-Aglaroxin C. To demonstrate the utility of the kinetic resolution methodology, we targeted asymmetric syntheses of the pyrimidone rocaglamide natural products (+)-aglaiaastatin (2) and (–)-aglaroxin C (3). The absolute configuration of (+)-aglaiaastatin (2) has been proposed to be identical to

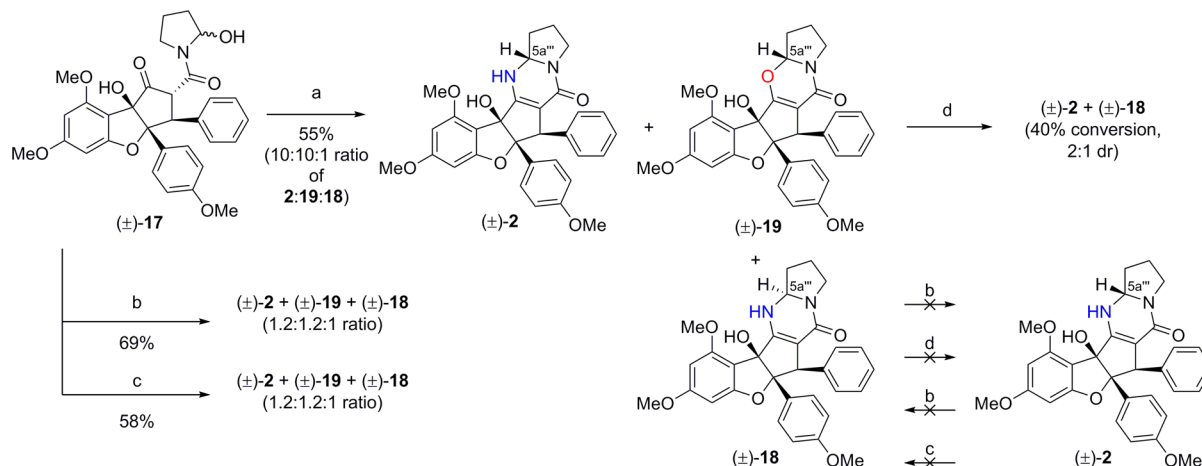
other members of the rocaglate family and circular dichroism spectra supports this notion.²¹ We intended to use our method to conclusively determine the absolute stereochemistry of 2 and to compare it to that of both (–)-ponapensin (4) and (–)-methyl rocaglate (1). The synthesis of aglaiaastatin (2, Scheme 1) involved base-mediated ketol rearrangement of

Scheme 1. Synthesis of (+)-Aglaiaastatin (2) and (–)-Aglaroxin C (3) from Hydrate (+)-5b



again (+)-5b to a keto-rocaglate intermediate followed by ester amide exchange to afford butyramide dimethyl acetal 16 similar to an intermediate employed by Watanabe and co-workers.²² Under acidic hydrolysis conditions, acetal 16 formed the hemiaminal derivative 17 (cf. Scheme 2) which was heated with ammonium acetate to form (+)-aglaiaastatin (2) ([α]_D²⁷ = +86.1° synthetic (c 0.7, CHCl₃), [α]_D²⁰ = +45.7° natural (c 0.19, CHCl₃)^{2b}) in 55% yield (10:1 dr, 4 steps). (–)-Aglaroxin C (3) ([α]_D²⁷ = –49.2° synthetic (c 0.1, CHCl₃), [α]_D²⁰ = –50.1° natural (c 0.41, CHCl₃)^{2b}) was obtained in 66% yield via dehydrogenation of (+)-aglaiaastatin (2) with DDQ. Interestingly, treatment of *epi*-aglaiaastatin 18 (cf. Scheme 2) with DDQ also provided aglaroxin C (3).

With (+)-aglaiaastatin (2) obtained in a 10:1 ratio to its C5a''' epimer 18 (*epi*-aglaiaastatin), we conducted a number of experiments to explain the high diastereoselectivity of the putative *N*-acyliminium cyclization. When hemiaminal 17 was heated at 60 °C for 2 h in the presence of ammonium acetate, we observed a 10:10:1 ratio of (±)-aglaiaastatin (2):oxazinone²³ (±)-19: C5a''' epimer (±)-18 (Scheme 2) in 55% yield. Furthermore, we found that (±)-19 could be synthesized directly by heating (±)-17 overnight in the presence of magnesium sulfate (42%).¹⁹ The structure of 19 and its configuration at C5a''' was determined via X-ray crystal structure analysis (Figure 4).¹⁹ When hemiaminal (±)-17 was treated with formic acid and ammonium formate at room temperature,²² we observed a 1.2:1.2:1 ratio of (±)-2:(±)-19:(±)-18 in 69% yield (Scheme 2). The product ratio seems to be controlled by the nature of the *N*-acyliminium counterion, as thermolysis of (±)-17 in the presence of ammonium formate led to the same distribution of products (Scheme 2). Epimer (±)-18 could not be converted to (±)-aglaiaastatin (2) when subjected to ammonium acetate/heat or ammonium formate/formic acid. Likewise, (±)-aglaiaastatin (2) could not be converted to (±)-*epi*-aglaiaastatin 18 through treatment with ammonium formate/formic acid or ammonium formate/heat. Interestingly, oxazinone (±)-19 was partially converted to (±)-aglaiaastatin (2) and (±)-*epi*-aglaiaastatin 18 in a 2:1 ratio

Scheme 2. Experiments To Probe the Mechanism of *N*-Acyliminium Cyclizations^a

^aConditions: (a) ammonium acetate (10 equiv), THF, 60 °C, 2 h; (b) formic acid (1 equiv), ammonium formate (15 equiv), THF, rt, 6 d (69% from (±)-5b; no conversion from (±)-2; (c) ammonium formate (10 equiv), THF, 60 °C, 12 h (58% from (±)-5b; no conversion from (±)-2); (d) ammonium acetate (10 equiv), THF, 60 °C, 12 h.

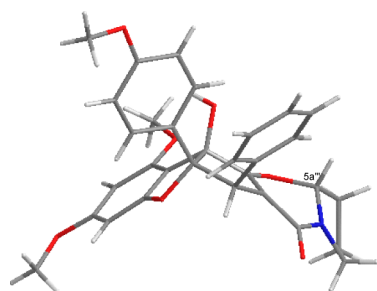


Figure 4. X-ray structure of oxazinone 19.

favoring (±)-2 when heated in the presence of ammonium acetate (60 °C, 12 h). Since the formation of aglaiastatin (2) and *epi*-aglaiastatin 18 is irreversible, the diastereoselectivity of these products may be controlled through the Curtin–Hammett principle²⁴ wherein cyclization occurs faster when the *N*-acyliminium reaction center is above the convex face of the rocaglate scaffold. Figure 5 shows ground state conformers of *N*-acyliminium intermediates leading to aglaiastatin (2) and *epi*-aglaiastatin 18 calculated in the gas phase using the B3LYP/6-31G* level of theory.¹⁷ These *N*-acyliminiums feature acetate counterions that are hydrogen-bonded to both the hydroxyl²⁵ and enamine on the convex face of the rocaglate scaffold. Intermediate 20a (leading to aglaiastatin) is 2.0 kcal/mol lower in energy than its corresponding rotamer 20b. This energetic difference appears to be due to steric repulsion between the 3''-methylene of the pyrrolidine and the acetate counterion, and the *N*-acyliminium reaction center residing within the concave face of the cyclopenta[*b*]benzofuran scaffold. Through invoking the Hammond postulate, these intermediates provide a rationale for the observed 10:1 diastereoselectivity using acetate as counterion. When rotamers 20a and 20b were subjected to a similar computation with formate as the counterion, the corresponding formate structures were found to have an energy difference of 1.0 kcal/mol,¹⁹ presumably because of the smaller counterion size. Furthermore, acetate is more basic than formate for deprotonation of the enamine as the nitrogen attacks the *N*-acyliminium. This explains the greater production of aglaiastatin (2) vs oxazinone 19 when acetate is the counterion as compared with formate (cf. Scheme 2). We also

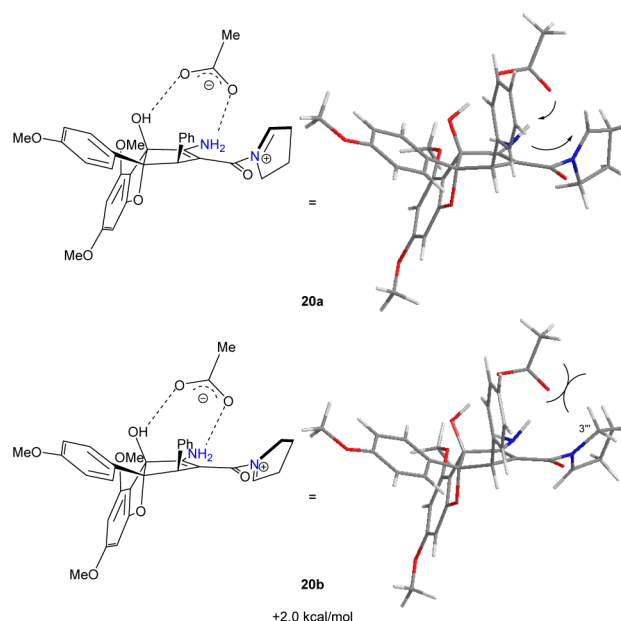


Figure 5. Ground state conformers (B3LYP/6-31G*) of *N*-acyliminium rotamers 20a and 20b.

considered that the *N*-acyliminium cyclization may also occur through 6 π -electrocyclization (Figure 6) in which formation of aglaiastatin (2) is torquoselective through the aforementioned steric effects.²⁶ However, this mechanism would require

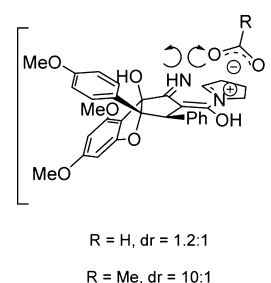
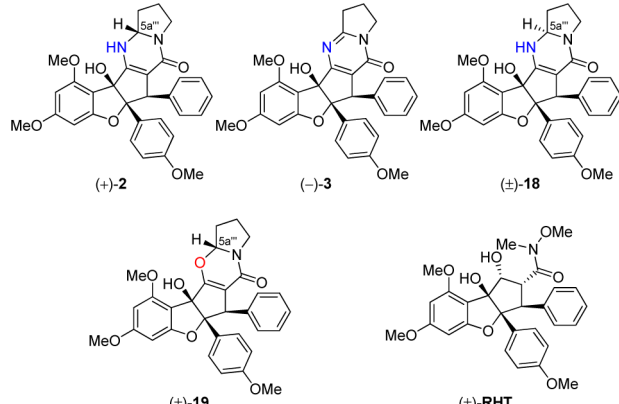


Figure 6. Alternative, torquoselective 6 π -electrocyclization.

tautomerization and flattening of the six participating atoms in order to achieve the orbital alignment necessary for electrocyclic cyclization.

Biological Evaluation. With the natural products (enantiopure and racemic) and analogues in hand, we tested their potencies in whole cell assays reporting on several of the biological activities previously reported for the rocaglate compound class: inhibition of the HSF1-dependent heat-shock response, cytotoxicity, and translation inhibition (Table 3).^{5b} Additionally, we synthesized the unnatural enantiomers of

Table 3. Concentration-Dependent Biological Activities of Aglaiastatin and Related Compounds in Whole Cells^a



entry	compound	heat-shock response IC ₅₀ , nM ^b	cytotoxicity IC ₅₀ , nM ^c	translation inhibition EC ₅₀ , nM ^d
1	(+)-2	3.8	3.9	15.6
2	(±)-2	5.2	7.1	26.0
3	(-)-3	15.3	11.2	77.7
4	(±)-18	23.8	21.7	117.6
5	(±)-19	25.8	31.8	241.1
6	(±)-3	37.7	26.1	210.7
7	(-)-2	99.2	105.7	761.8
8	(+)-3	>1000	>1000	>1000
9	(±)-RHT	14.8	18.5	75.6

^aFour-parameter nonlinear curve fit of dose–response data in whole cell assays, all determinations in quadruplicate. $R^2 > 0.95$ for all curve fits. ^bConcentration resulting in 50% reduction in heat-induced luciferase reporter activity. ^cConcentration resulting in 50% reduction in relative viable cell number. ^dConcentration resulting in half-maximal inhibition of constitutive luciferase activity.

aglaiastatin (**2**) and aglaroxin C (**3**) by using the (*S,S*) enantiomer of Rh(III) diphenylethylenediamine **A** in the kinetic resolution of substrate (**±**)-**5b** (cf. Table 1 and Scheme 1), and tested (–)-aglaiastatin (**2**) and (+)-aglaroxin C (**3**) in the aforementioned assays. Figure 5 summarizes the data. The natural enantiomer, (+)-aglaiastatin (**2**) was found to be the most potent with single-digit nanomolar IC₅₀ values obtained for both heat-shock reporter inhibition and cytotoxicity (entry 1). The racemates of aglaiastatin (**2**, entry 2) and aglaroxin C (**3**, entry 6) were not as potent as their respective natural enantiomers (entries 1 and 3, respectively), and unnatural enantiomers (entries 7 and 8, respectively) were significantly less potent. Interestingly, (+)-**2** and (±)-**2** (entries 1 and 2, respectively) were more potent than the positive control rohinitib (**RHT**, entry 9), and natural aglaroxin C ((–)-**3**, entry 3) was found to have similar potencies as **RHT**. Of note, (–)-**2**

retains moderate bioactivity suggesting the possibility of an alternative molecular target(s).²⁷ In general, (±)-*epi*-aglaiastatin (**18**, entry 4) was more potent than (±)-aglaroxin C (**3**, entry 6), which was more potent than oxazinone (±)-**19** (entry 5).

CONCLUSION

In summary, we have accomplished a highly enantio- and diastereoselective kinetic resolution of aglain ketones using Rh(III)-mediated transfer hydrogenation. This process allows rapid access to bioactive rocaglate natural products in a biomimetic fashion. From the substrate scope, it is also evident that this process can be used to access a variety of enantiopure aglain and rocaglate analogues. We further demonstrated the utility of the methodology by enantioselective syntheses of (+)-aglaiastatin (**2**) and (–)-aglaroxin C (**3**). Finally, we tested both enantiomers of aglaiastatin (**2**) and aglaroxin C (**3**) for several of the most prominent bioactivities reported for this compound class and found that the natural enantiomers were most potent. Moreover, we observed a concordance in potency for all derivatives across the three bioassays, suggesting there may be a single, conserved molecular target responsible for their activity. Further work toward the synthesis and biological evaluation of aglaiastatin and rocaglate analogs is currently in progress and will be reported in due course.

ASSOCIATED CONTENT

Supporting Information

Experimental procedures and characterization data for all new compounds described herein, including a CIF file for compound **19**. This material is available free of charge via the Internet at <http://pubs.acs.org>.

AUTHOR INFORMATION

Corresponding Author

porco@bu.edu

Author Contributions

[†]S.D.S. and N.J.L. contributed equally.

Notes

The authors declare no competing financial interest.

ACKNOWLEDGMENTS

We thank the National Institutes of Health (R01 GM073855 and R01 CA175744) for research support, Dr. Jeffrey Bacon (Boston University) for X-ray crystal structure analyses, and Dr. Norman Lee (Boston University) for high-resolution mass spectrometry data. NMR (CHE-0619339) and MS (CHE-0443618) facilities at Boston University are supported by the NSF. Research at the Center for Chemical Methodology and Library Development at Boston University (CMLD-BU) was supported by NIH grant GM-067041. We also thank Professor John Snyder (Boston University), Prof. Amir Hoveyda (Boston College), Mr. Tian Qin (Boston University), Ms. Sarah Skrabajoiner (University of New Hampshire), and Mr. Wenyu Wang (Boston University) for extremely helpful and stimulating discussions.

REFERENCES

- (1) Ko, F.; Wu, T.; Liou, M.; Huang, T.; Teng, C. *Eur. J. Pharmacol.* **1992**, 218, 129–135.
- (2) (a) Ohse, T.; Ohba, S.; Yamamoto, T.; Koyano, T.; Umezawa, K. *J. Nat. Prod.* **1996**, 59, 650. (b) Nugroho, B. W.; Edrada, R. A.;

- Güssregen, B.; Wray, B.; Witte, L.; Proksch, P. *Phytochemistry* **1997**, *44*, 1455–1461.
- (3) Kokpol, U.; Venaskulchai, B.; Simpson, J.; Weavers, R. T. *J. Chem. Soc., Chem. Commun.* **1994**, 773–774.
- (4) Salim, A.; Pawlus, A.; Chai, H.; Farnsworth, N.; Kinghorn, A. D.; Carcache-Blanco, E. *Bioorg. Med. Chem. Lett.* **2007**, *17*, 109–112.
- (5) (a) Lee, S.; Cui, B.; Mehta, R.; Kinghorn, A. D.; Pezzuto, J. *Chem. Biol. Interact.* **1998**, *115*, 215–228. (b) Santagata, S.; Mendillo, M. L.; Tang, Y.; Subramanian, A.; Perley, C. C.; Roche, S. P.; Wong, B.; Narayan, R.; Kwon, H.; Koeva, M.; Amon, A.; Golub, T. R.; Porco, J. A., Jr.; Whitesell, L.; Lindquist, S. *Science* **2013**, *341*, No. 1238303. (c) Emhemmed, F.; Ali Azouaou, S.; Thuaud, F.; Schini-Kerth, V.; Désaubry, L.; Muller, C. D.; Fuhrmann, G. *Biochem. Pharmacol.* **2014**, *89*, 185–196. (d) Saolmé, C.; Ribeiro, N.; Chavagnan, T.; Thuaud, F.; Serova, M.; de Gramont, A.; Faivre, S.; Raymond, E.; Désaubry, L. *Eur. J. Med. Chem.* **2014**, *81*, 189–191. (e) Boussemart, L.; Malka-Mahieu, H.; Girault, I.; Allard, D.; Hemmingsson, O.; Tomasic, G.; Thomas, M.; Basmadjian, C.; Riebeiro, N.; Thuaud, F.; Mateus, C.; Routier, E.; Kamsu-Kom, N.; Agoussi, S.; Eggermont, A. M.; Désaubry, L.; Robert, C.; Vagner, S. *Nature* **2014**, *513*, 105–109. (f) Callahan, K.; Minhajuddin, M.; Corbett, C.; Lagadinou, E.; Rossi, R.; Balys, M.; Pan, L.; Jacob, S.; Frontier, A.; Grever, M.; Lucas, D.; Kinghorn, A. D.; Liesveld, J. L.; Becker, M.; Jordan, C. *Leukemia* **2014**, *28*, 1960–1968.
- (6) Baumann, B.; Bohnenstengel, F.; Siemund, D.; Wajant, H.; Weber, C.; Herr, I.; Debatin, K.-M.; Proksch, P.; Wirth, T. *J. Biol. Chem.* **2002**, *277*, 44791–44800.
- (7) Fahrig, T.; Geralch, I.; Horvath, E. *Mol. Pharmacol.* **2005**, *67*, 1544–1555.
- (8) Bernard, Y.; Ribeiro, N.; Thuaud, F.; Turkeri, G.; Dirr, R.; Boulberdaa, M.; Nebigil, C. G.; Désaubry, L. *PLoS One* **2011**, *6*, e25302.
- (9) Lajkiewicz, N. J.; Cognetta, A. B., III; Niphakis, M. J.; Cravatt, B. F.; Porco, J. A., Jr. *J. Am. Chem. Soc.* **2014**, *136*, 2659–2664.
- (10) Biosynthetic hypothesis for aglains and rocaglates: (a) Bacher, M.; Hofer, O.; Brader, G.; Vajrodaya, S.; Greger, H. *Phytochemistry* **1999**, *52*, 253. For reviews on the isolation, pharmacological activity, and synthesis of flavaglines, see: (b) Ebada, S. S.; Lajkiewicz, N.; Porco, J. A., Jr.; Li-Weber, M.; Proksch, P. *Prog. Chem. Org. Nat. Prod.* **2011**, *94*, 1–58. (c) Basamadjian, C.; Thuaud, F.; Ribeiro, N.; Désaubry, L. *Future Med. Chem.* **2013**, *5*, 2185–2197. (d) Pan, L.; Woodard, J. L.; Lucas, D. M.; Fuchs, J. R.; Kinghorn, A. D. *Nat. Prod. Rep.* **2014**, *31*, 924–939.
- (11) Total syntheses and absolute configuration assignments of (+)-ponapensin and (+)-elliptifoline: (a) Lajkiewicz, N. J.; Roche, S. P.; Gerard, B.; Porco, J. A., Jr. *J. Am. Chem. Soc.* **2012**, *134*, 13108–13113. isolation report for (–)-elliptifoline: (b) Wang, S.-K.; Cheng, Y. J.; Duh, C.-Y. *J. Nat. Prod.* **2001**, *64*, 92–94.
- (12) For references on kinetic resolutions of racemic, bridged ketones via biosynthetic reductions, see: (a) Nakazaki, M.; Chikamatsu, H.; Naemura, K.; Nishino, M.; Murakami, H.; Asao, M. *J. Org. Chem.* **1979**, *44*, 4588–4593. (b) Truppo, M. D.; Kim, J.; Brower, M.; Madin, A.; Sturr, M. G.; Moore, J. C. *J. Mol. Catal. B: Enzymology* **2006**, *38*, 158–162.
- (13) (a) Miller, L. C.; Ndungu, M.; Sarpong, R. *Angew. Chem., Int. Ed.* **2009**, *48*, 2398–2402. (b) Kamlet, A. S.; Preville, C.; Farley, K. A.; Piotrowski, D. W. *Angew. Chem., Int. Ed.* **2013**, *52*, 10607–10610.
- (14) (a) Hashiguchi, S.; Fujii, A.; Haack, K.; Matsumura, K.; Ikariya, T.; Noyori, R. *Angew. Chem., Int. Ed.* **1997**, *36*, 288–290. (b) Noyori, R.; Hashiguchi, S. *Acc. Chem. Res.* **1997**, *30*, 97–102.
- (15) Lemke, M.; Schwab, P.; Fischer, P.; Tischer, S.; Witt, M.; Noehringer, L.; Rogachev, V.; Jäger, A.; Kataeva, O.; Frölich, R.; Metz, P. *Angew. Chem., Int. Ed.* **2013**, *52*, 11651–11655.
- (16) (a) Yamakawa, M.; Yamada, I.; Noyori, R. *Angew. Chem., Int. Ed.* **2001**, *40*, 2818–2821. (b) Soni, R.; Collinson, J.-M.; Clarkson, G. C.; Wills, M. *Org. Lett.* **2011**, *13*, 4304–4307.
- (17) Computational analysis was performed using *Spartan '10* from Wavefunction, Inc., Irvine, CA.
- (18) Thuaud, F.; Ribeiro, N.; Gaiddon, C.; Cresteil, T.; Desaubry, L. *J. Med. Chem.* **2010**, *54*, 411–415.
- (19) Please see Supporting Information for complete experimental details.
- (20) Zondlo, N. J. *Acc. Chem. Res.* **2013**, *46*, 1039–1049.
- (21) Greger, H.; Pacher, T.; Brem, B.; Bacher, M.; Hofer, O. *Phytochemistry* **2001**, *57*, 57–64.
- (22) Watanabe, T.; Takeuchi, T.; Kohzuma, S.; Umezawa, K.; Otsuka, M. *Chem. Commun.* **1998**, 1097–1098.
- (23) (a) Karadogan, B.; Parsons, P. J. *Tetrahedron* **2001**, *57*, 8699–8703. (b) Modak, A.; Dutta, U.; Kancherla, R.; Maity, S.; Bhadra, M.; Mobin, S. M.; Maiti, D. *Org. Lett.* **2014**, *16*, 2602–2605.
- (24) Hauptert, L. J.; Poutsma, J. C.; Wenthold, P. G. *Acc. Chem. Res.* **2009**, *42*, 1480–1488.
- (25) (a) Li, X.; Liu, P.; Houk, K. N.; Birman, V. B. *J. Am. Chem. Soc.* **2008**, *130*, 13836–13837. (b) Liu, P.; Yang, X.; Birman, V. B.; Houk, K. N. *Org. Lett.* **2012**, *14*, 3288–3291.
- (26) Patel, A.; Barcan, G. A.; Kwon, O.; Houk, K. N. *J. Am. Chem. Soc.* **2013**, *135*, 4878–4883.
- (27) Polier, G.; Neumann, J.; Thuaud, F.; Ribeiro, N.; Gelhaus, C.; Schmidt, H.; Giaisia, M.; Köhler, R.; Müller, W. W.; Proksch, P.; Leippe, M.; Janssen, O.; Désaubry, L.; Krammer, P. H.; Li-Weber, M. *Chem. Biol.* **2012**, *19*, 1093–1104.